Int. J. Solids Structures Vol. 28, No. 3, pp. 373–383, 1991
Printed in Great Britain.

0020-7683/91 $3.00 + .00

MODELING OF DELAMINATION IN COMPOSITE LAMINATES USING A LAYER-WISE PLATE THEORY

E. J. BARBERO† and J. N. REDDY‡
Department of Engineering Science and Mechanics, Virginia Polytechnic Institute and State University, Blacksburg, VA 24061-0219, U.S.A.

(*Received* 20 *June* 1990; *in revised form* 30 *November* 1990)

Abstract—The layer-wise laminate theory of Reddy is extended to account for multiple delaminations between layers, and the associated computational model is developed. Delaminations between layers of composite plates are modeled by jump discontinuity conditions at the interfaces. Geometric nonlinearity is included to capture layer buckling. The strain energy release rate distribution along the boundary of delaminations is computed by a novel algorithm. The computational model presented is validated through several numerical examples.

1. INTRODUCTION

The objective of this study is to characterize delaminations in laminated composite plates using a layer-wise theory. We wish to raise the quality of the analysis beyond that provided by conventional, equivalent single-layer laminate theories without resorting to a full three-dimensional analysis. A computational model based on the layer-wise theory of Reddy (1987) is presented, and the model is used in the analysis of plates with delaminations.

The advantages of an equivalent single-layer theory over a 3-D analysis are many. In the application of 3-D finite elements to bending of plates, the aspect ratio of the elements must be kept to a reasonable value in order to avoid shear locking. If the laminate is modeled with 3-D elements, an excessively refined mesh in the plane of the plate needs to be used because the thickness of an individual lamina dictates the aspect ratio of an element. On the other hand, a finite element model based on a laminate theory does not have the same aspect ratio limitation because the thickness dimension is eliminated by integrating through the laminate thickness. However, the hypothesis commonly used in the conventional (ie., both classical and shear deformation) laminate theories leads to a poor representation of strains in cases of interest, namely, in thick composite laminates with dissimilar material layers.

A 2-D laminate theory that provides a compromise between the 3-D theory and conventional plate theories is the layer-wise laminate theory of Reddy (1987), with layer-wise continuous representation of displacements through the thickness. Although this theory is computationally more expensive than the conventional laminate theories, it predicts the interlaminar stresses very accurately (Reddy *et al.*, 1989; Barbero *et al.*, 1990a,b). Furthermore, it has the advantage of all plate theories in the sense that it is a two-dimensional theory, and does not suffer from aspect ratio limitations associated with 3-D finite element models.

The layer-wise representation of the displacements through the thickness has proven to be successful. Yu (1959) and Durocher and Solecki (1975) considered the case of a three-layer plate. Mau (1973), Srinivas (1973), Sun and Whitney (1972), and Seide (1980) derived theories for layer-wise linear displacements. Reissner's mixed variational principle was used by Murakami (1986) and Toledano and Murakami (1987) to include the interlaminar stresses as primary variables. Both continuous functions and piece-wise linear functions were used. Reddy's theory is chosen in this work because of the generality it offers in modeling delaminations.

Delaminations between laminae are common defects in laminates, usually developed

† Presently Assistant Professor, Department of Mechanical and Aerospace Engineering, West Virginia University, Morgantown, WV, U.S.A.
‡ Clifton C. Garvin Professor.

either during manufacturing or during operational life of the laminate (e.g., fatigue, impact). Delaminations may buckle and grow in panels subjected to in-plane compressive loads. Delaminated panels have reduced load-carrying capacity in both the pre- and post-buckling regimes. However, under certain circumstances, the growth of delaminations can be arrested. An efficient use of laminated composite structures requires an understanding of the delamination onset and growth. An analysis methodology is necessary to model composite laminates in the presence of delaminations.

Self-similar growth of the delamination along an interface between layers is suggested by the laminated nature of the panel. It was noted by Obreimoff (1980) and Inoue and Kobatake (1959) that axial compressive load applied in the direction of the delamination promotes further growth in the same direction. One-dimensional and two-dimensional models for the delamination problem were proposed by Chai (1982), Simitses *et al.* (1985), Kachanov (1976), Ashizawa (1981), and Sallam and Simitses (1985). According to these models, the delamination can grow only after the debonded portion of the laminate buckles. However, the delamination can also grow due to shear modes II and III.

The spontaneous growth of a delamination while the applied load is constant is called "unstable growth". If the load has to be increased to promote further delamination, the growth is said to be "stable growth". The onset of delamination growth can be followed by stable growth, or unstable indefinite growth or even unstable growth followed by arrest and subsequent stable growth.

In most studies the buckling load of the debonded laminate is calculated using bifurcation analysis (see Chai, 1982; Simitses *et al.*, 1985; Webster, 1981; Bottega and Maewal, 1983). Bifurcation analysis is not appropriate for debonded laminates that have bending–extension coupling, as noted by Simitses *et al.* (1985). Even laminates that are originally symmetric, once delaminated, experience bending–extension coupling. In general, delaminations are unsymmetrically located with respect to the midplane and the resulting delaminated layers become unsymmetric. Therefore, in-plane compressive load produces lateral deflection and the primary equilibrium path is not trivial ($w \neq 0$). Furthermore, bifurcation analysis does not permit computation of the strain energy release rate.

Nonlinear plate theories have been used to analyze the post-buckling behavior of debonded laminates. Bottega and Maewal (1985), Yin (1985), and Fei and Yin (1985) analyzed the problem of a circular plate with concentric, circular delamination. The von Kármán type of nonlinearity has been used in these studies.

Most of the analyses performed have been restricted to relatively simple models. The material was assumed to be isotropic in most cases and orthotropic in a few, thus precluding the possibility of analyzing the influence of the stacking sequence and bending–extension coupling.

The Rayleigh–Ritz method has been used by Chai (1982), Chai *et al.* (1981), and Shivakumar and Whitcomb (1985) to obtain approximate solutions to simple problems. Orthotropic laminates were considered by Chai and Babcock (1985) and circular delaminations by Webster (1981).

The finite element method was used by Whitcomb (1981) to analyze through-width delaminated coupons. Plane-strain elements were used to model sections of beams, or plates in cylindrical bending. The analysis of delaminations of arbitrary shape in panels requires the use of three-dimensional elements, with a considerable computational cost. A three-dimensional, fully nonlinear finite element analysis was used by Whitcomb (1988), where it was noted that "... plate analysis is potentially attractive because it is inherently much less expensive than 3D analysis." Plate elements and multi-point constraints (MPC) have been used by Whitcomb and Shivakumar (1987) to study delamination buckling and by Wilt *et al.* (1988) to study free-edge delaminations. This approach is inconvenient in many situations. First, the MPC approach requires a large number of nodes to simulate actual contact between laminae. Second, a new plate element is added for each delamination. The MPC approach becomes too complex for the practical situation of multiple delaminations through the thickness. Third, all plate elements have their middle surface in the same plane, which is unrealistic for the case of delaminated laminae that have their middle surface at different locations through the thickness of the plate.

The layer-wise theory of Reddy (1987) is extended here to model the kinematics of multiple delaminations. The theory is applied to embedded delaminations that are entirely separated from the base laminate after buckling. Numerical results are presented for a number of problems and the results are compared to existing solutions.

2. THE LAYER-WISE LAMINATE PLATE THEORY

Increased use of laminated composite plates has motivated the development of refined plate theories to overcome certain shortcomings of the classical laminate theory. The first-order and higher-order shear deformation theories (see Reddy, 1984, 1989, 1990) yield improved global response, such as maximum deflections, natural frequencies and critical buckling loads. Conventional theories based on a single continuous and smooth displacement field through the thickness of a composite laminate give poor estimation of the interlaminar stresses. Since important modes of failure are related to interlaminar stresses, refined plate theories that can model the local behavior of the plate more accurately are required. The layer-wise plate theory is shown to provide excellent predictions of the local response, i.e., interlaminar stresses, in-plane displacements and stresses, etc. (Barbero, 1989). This is due to the refined representation of the laminated nature of composite plates provided by the theory and to the consideration of shear deformation effects. Before we present the theory for delamination modeling, a review of the basic elements of the theory is first presented.

Consider a laminated plate composed of N orthotropic laminae, each being oriented arbitrarily with respect to the laminate (x, y) coordinates, which are taken to be in the midplane of the laminate. The displacements (u_1, u_2, u_3) at a point (x, y, z) in the laminate are assumed to be of the form (see Reddy, 1987),

$$\begin{aligned} u_1(x, y, z) &= u(x, y) + U(x, y, z) \\ u_2(x, y, z) &= v(x, y) + V(x, y, z) \\ u_3(x, y, z) &= w(x, y), \end{aligned} \tag{1}$$

where (u, v, w) are the displacements of a point $(x, y, 0)$ on the reference plane of the laminate, and U and V are functions which vanish on the reference plane:

$$U(x, y, 0) = V(x, y, 0) = 0. \tag{2}$$

In order to reduce the three-dimensional theory to a two-dimensional one, Reddy (1987) suggested layer-wise approximation of the variation of U and V with respect to the thickness coordinate, z:

$$\begin{aligned} U(x, y, z) &= \sum_{j=1}^{n} u^j(x, y)\phi^j(z) \\ V(x, y, z) &= \sum_{j=1}^{n} v^j(x, y)\phi^j(z), \end{aligned} \tag{3}$$

where u^j and v^j are undetermined coefficients and ϕ^j are any piece-wise continuous functions that satisfy the condition

$$\phi^j(0) = 0 \quad \text{for all} \quad j = 1, 2, \ldots, n. \tag{4}$$

The approximation in eqn (3) can also be viewed as the global semi-discrete finite-element approximations (Reddy, 1984), through the thickness. In that case ϕ^j denote the global interpolation functions, and u^j and v^j are the global nodal values of U and V (and possibly their derivatives) at the nodes through the thickness of the laminate.

3. A MODEL FOR THE STUDY OF DELAMINATIONS

3.1. *Introduction*

Delamination buckling in laminated plates subjected to in-plane compressive loads is well recognized as a limiting factor on the performance of composite structures. While the accuracy of the analysis is of paramount importance to the correct evaluation of damage in composites, the cost of analysis precludes the use of three-dimensional models. This section deals with the formulation of a laminated plate theory that can handle multiple delaminations in composite plates.

3.2. *Formulation of the theory*

Modeling of delaminations in laminated composite plates requires an appropriate kinematical description to allow for separation and slipping. This can be incorporated into the layer-wise theory by proper modification of the expansion of the displacements (1) through the thickness. The layer-wise theory can be extended to model the kinematics of a layered plate, with provision for delaminations, by using the following expansion of the displacements through the thickness of the plate:

$$\begin{aligned} u_1(x,y,z) &= u(x,y) + \sum_{j=1}^{N} \phi^j(z) u^j(x,y) + \sum_{j=1}^{D} H^j(z) U^j(x,y) \\ u_2(x,y,z) &= v(x,y) + \sum_{j=1}^{N} \phi^j(z) v^j(x,y) + \sum_{j=1}^{D} H^j(z) V^j(x,y) \\ u_3(x,y,z) &= w(x,y) + \sum_{j=1}^{D} H^j(z) W^j(x,y) \end{aligned} \tag{5}$$

where the step functions H^j are computed in terms of the Heaviside step functions $\hat{H}$ as:

$$\begin{aligned} H^j(z) &= \hat{H}(z-z_j) = 1 \quad \text{for} \quad z \geqslant z_j \\ H^j(z) &= \hat{H}(z-z_j) = 0 \quad \text{for} \quad z < z_j. \end{aligned} \tag{6}$$

In eqn (5) $\phi^j(z)$ are linear Lagrange interpolation functions, N is the number of layers used to model the laminate and D is the number of delaminations. The jumps in the displacements at the jth delaminated interface are given by U^j, V^j and W^j. Using the step functions $H^j(z)$, we can model any number of delaminations through the thickness; the number of additional variables is equal to the number of delaminations considered. At delaminated interfaces, the displacements on adjacent layers remain independent, allowing for separation and slipping.

Although nonlinear effects are important, rotations and displacements are not expected to be so large as to require a full nonlinear analysis. Only the von Kármán nonlinearity in the kinematic equations needs to be considered.

The linear strains of the theory are

$$\varepsilon_x = \frac{\partial u}{\partial x} + \sum_j^N \phi^j \frac{\partial u^j}{\partial x} + \underline{\sum_j^D H^j \frac{\partial U^j}{\partial x}}$$

$$\varepsilon_y = \frac{\partial v}{\partial y} + \sum_j^N \phi^j \frac{\partial v^j}{\partial x} + \underline{\sum_j^D H^j \frac{\partial V^j}{\partial x}}$$

$$\varepsilon_{xy} = \frac{1}{2}\left(\frac{\partial u}{\partial y} + \frac{\partial v}{\partial x}\right) + \frac{1}{2}\sum_j^N \phi^j \left(\frac{\partial u^j}{\partial y} + \frac{\partial v^j}{\partial x}\right) + \underline{\frac{1}{2}\sum_j^D H^j \left(\frac{\partial U^j}{\partial y} + \frac{\partial V^j}{\partial x}\right)} \tag{7}$$

$$\varepsilon_z = 0 \quad \text{because} \quad \frac{\partial H^j}{\partial z} = 0$$

$$\varepsilon_{xz} = \frac{1}{2}\left[\frac{\partial w}{\partial x} + \sum_j^N \frac{\partial \phi^j}{\partial z} u^j + \underline{\sum_j^D H^j \frac{\partial W^j}{\partial x}}\right]$$

$$\varepsilon_{yz} = \frac{1}{2}\left[\frac{\partial w}{\partial y} + \sum_j^N \frac{\partial \phi^j}{\partial z} v^j + \underline{\sum_j^D H^j \frac{\partial W^j}{\partial y}}\right] \tag{8}$$

where the underlined terms are due to the introduction of the delamination variables U^j, V^j, W^j.

The nonlinear portion of the strains are:

$$\eta_x = \frac{1}{2}\left(\frac{\partial w}{\partial x}\right)^2 + \underline{\frac{1}{2}\sum_i^D \sum_j^D \left(H^i H^j \frac{\partial W^i}{\partial x}\frac{\partial W^j}{\partial x}\right)} + \underline{\frac{\partial w}{\partial x}\sum_i^D H^i \frac{\partial W^i}{\partial x}}$$

$$\eta_y = \frac{1}{2}\left(\frac{\partial w}{\partial y}\right)^2 + \underline{\frac{1}{2}\sum_i^D \sum_j^D \left(H^i H^j \frac{\partial W^i}{\partial y}\frac{\partial W^j}{\partial y}\right)} + \underline{\frac{\partial w}{\partial y}\sum_i^D H^i \frac{\partial W^i}{\partial y}}$$

$$\eta_{xy} = \frac{1}{2}\frac{\partial w}{\partial x}\frac{\partial w}{\partial y} + \underline{\frac{1}{2}\sum_i^D \sum_j^D \left(H^i H^j \frac{\partial W^i}{\partial x}\frac{\partial W^j}{\partial y}\right) + \frac{1}{2}\frac{\partial w}{\partial x}\sum_j^D \left(H^j \frac{\partial W^j}{\partial y}\right) + \frac{1}{2}\frac{\partial w}{\partial y}\sum_i^D \left(H^i \frac{\partial W^i}{\partial x}\right)} \tag{9}$$

$$\eta_{xz} = \eta_{yz} = \eta_z = 0.$$

The virtual strain energy is now given by

$$\delta U = \delta U_{CL} + \delta U_{CNL} + \delta U_{DL} + \delta U_{DNL} \tag{10a}$$

where

δU_{CL} is the contribution of the classical linear terms
δU_{CNL} is the contribution of the von Kármán classical nonlinear terms
δU_{DL} is the contribution of the new linear terms [underlined in eqn (8)]
δU_{DNL} is the contribution of the new nonlinear terms [underlined in eqn (9)]. (10b)

The contribution of the conventional displacements to linear terms is:

$$\delta U_{CL} = \int_\Omega \left\{N_x \frac{\partial \delta u}{\partial x} + \sum_{j=1}^N N_x^j \frac{\partial \delta u^j}{\partial z} + N_y \frac{\partial \delta u}{\partial y} + \sum_{j=1}^N N_y^j \frac{\partial \delta v^j}{\partial x} + N_{xy}\left(\frac{\partial \delta u}{\partial y} + \frac{\partial \delta v}{\partial x}\right)\right.$$
$$\left. + \sum_{j=1}^N N_{xy}^j \left(\frac{\partial u^j}{\partial y} + \frac{\partial v^j}{\partial x}\right) + Q_x \frac{\partial \delta w}{\partial x} + \sum_{j=1}^N Q_x^j u^j + Q_y \frac{\partial \delta w}{\partial y} + \sum_{j=1}^N Q_y^j v^j - q\delta w\right\} dA. \tag{11}$$

The contribution of the von Kármán nonlinear terms is

$$\delta U_{CNL} = \int_\Omega \left\{N_x \frac{\partial w}{\partial x}\frac{\partial \delta w}{\partial x} + N_y \frac{\partial w}{\partial y}\frac{\partial \delta w}{\partial y} + N_{xy}\left(\frac{\partial w}{\partial x}\frac{\partial \delta w}{\partial y} + \frac{\partial \delta w}{\partial x}\frac{\partial w}{\partial y}\right)\right\} dA. \tag{12}$$

The contribution of the new linear terms is

$$\delta U_{DL} = \sum_{i=1}^{D} \int_{\Omega} \left\{ \hat{Q}_x^i \frac{\partial \delta W^i}{\partial x} + \hat{Q}_y^i \frac{\partial \delta W^i}{\partial y} + M_x^i \frac{\partial \delta U^i}{\partial x} + M_y^i \frac{\partial \delta V^i}{\partial y} + M_{xy}^i \left(\frac{\partial \delta U^i}{\partial y} + \frac{\partial \delta V^i}{\partial x} \right) \right\} dx\, dy \tag{13a}$$

where

$$(\hat{Q}_x^i, \hat{Q}_y^i) = \int_{-h/2}^{h/2} (\sigma_{xz}, \sigma_{yz}) H^i(z)\, dz$$

$$(M_x^i, M_y^i, M_{xy}^i) = \int_{-h/2}^{h/2} (\sigma_x, \sigma_y, \sigma_{xy}) H^i(z)\, dz. \tag{13b}$$

The contribution of the new nonlinear terms is

$$\begin{aligned} \delta U_{DNL} = \int_{\Omega} \Bigg\{ \sum_{i}^{D} \Bigg[& M_x^i \left(\frac{\partial w}{\partial x} \frac{\partial \delta W^i}{\partial x} + \frac{\partial \delta w}{\partial x} \frac{\partial W^i}{\partial x} \right) + M_y^i \left(\frac{\partial w}{\partial y} \frac{\partial \delta W^i}{\partial y} + \frac{\partial \delta w}{\partial y} \frac{\partial W^i}{\partial y} \right) \\ & + M_{xy}^i \left(\frac{\partial w}{\partial x} \frac{\partial \delta W^i}{\partial y} + \frac{\partial \delta w}{\partial x} \frac{\partial W^i}{\partial y} + \frac{\partial w}{\partial y} \frac{\partial \delta W^i}{\partial x} + \frac{\partial \delta w}{\partial y} \frac{\partial W^i}{\partial x} \right) \Bigg] + \sum_{i}^{D} \sum_{j}^{D} \tfrac{1}{2} M_x^{ij} \\ & \times \left(\frac{\partial W^i}{\partial x} \frac{\partial \delta W^j}{\partial x} + \frac{\partial \delta W^i}{\partial x} \frac{\partial W^j}{\partial x} \right) + \tfrac{1}{2} M_y^{ij} \left(\frac{\partial W^i}{\partial y} \frac{\partial \delta W^j}{\partial y} + \frac{\partial \delta W^i}{\partial y} \frac{\partial W^j}{\partial y} \right) \\ & + M_{xy}^{ij} \left(\frac{\partial W^i}{\partial y} \frac{\partial \delta W^j}{\partial x} + \frac{\partial W^j}{\partial x} \frac{\partial \delta W^i}{\partial y} \right) \Bigg\} d\Omega \end{aligned} \tag{14a}$$

where

$$(M_x^{ij}, M_y^{ij}, M_{xy}^{ij}) = \int_{-h/2}^{h/2} (\sigma_x, \sigma_y, \sigma_{xy}) H^i(z) H^j(z)\, dz. \tag{14b}$$

The boundary conditions of the theory are given below:

Geometric	Force
u	$N_x n_x + N_{xy} n_y$
v	$N_{xy} n_x + N_y n_y$
w	$Q_x n_x + Q_y n_y$
u^j	$N_x^j n_x + N_{xy}^j n_x$
v^j	$N_{xy}^j n_x + N_y^j n_y$
U^j	$M_x^j n_x + M_{xy}^j n_y$
V^j	$M_{xy}^j n_x + M_y^j n_y$
W^j	$\hat{Q}_{xz}^j n_x + \hat{Q}_{yz}^j n_y$.

(15)

The laminate constitutive equations can be obtained in the usual manner (see Reddy, 1988; Barbero, 1989).

3.3. *Fracture mechanics analysis*

The deformation field obtained from the layer-wise theory is used to compute the strain energy release rates along the boundary of the delamination. Delminations usually exhibit planar growth, i.e., the crack grows in its original plane. However, the shape of the crack

may vary with time. For example, a crack shape initially elliptic usually grows with variable aspect ratio. Therefore, the crack growth is not self-similar. However, a self-similar virtual crack extension will be assumed in order to compute the distribution of the strain energy release rate $G(s)$ along the boundary of the delamination.

The virtual crack extension method postulates that the strain energy release rate can be computed from the strain energy U and the representative crack length a as:

$$G(s) = \mathrm{d}U/\mathrm{d}a. \tag{16}$$

In the actual implementation of the virtual crack extension method, however, eqn (16) is approximated by a quotient $\Delta U/\Delta a$ that in the limit approximates the value of the strain energy release rate G. In the Jacobian derivative method (Barbero and Reddy, 1990), the $G(s)$ is computed without approximating the derivative, so it does not require that we choose the magnitude of the virtual crack extension Δa.

The boundary of a delamination is modeled as boundary conditions on the delamination variables U^I, V^I, and W^I, by setting them to zero. A self-similar virtual crack extension of the crack (delamination) is specified for the nodes on the boundary of the delamination, i.e., the two components of the normal to the delamination boundary are specified for each node on the boundary. The JDM is then used at each configuration (or load step) to compute $G(s)$ from the displacement field.

3.4. *Finite-element model*

The generalized displacements $(u, v, w, u^I, v^I, U^I, V^I, W^I)$ are expressed over each element as a linear combination of the two-dimensional interpolation functions ψ_i and the nodal values $(u_i, v_i, w_i, u_i^I, v_i^I, U_i^I, V_i^I, W_i^I)$ as follows:

$$(u, v, w, u^I, v^I, U^I, V^I, W^I) = \sum_{i=1}^{m} (u_i, v_i, w_i, u_i^I, v_i^I, U_i^I, V_i^I, W_i^I)\psi_i \tag{17}$$

where m is the number of nodes per element. Using eqn (17) in eqn (10a), we obtain the following finite element equations:

$$\begin{bmatrix} k^{11} & k_1^{12} & \dots & k_N^{12} & k_1^{13} & \dots & k_D^{13} \\ k_1^{21} & k_{11}^{22} & \dots & k_{1N}^{22} & k_{11}^{23} & \dots & k_{1D}^{23} \\ \vdots & \vdots & & \vdots & \vdots & & \vdots \\ k_N^{21} & k_{N1}^{22} & \dots & k_{NN}^{22} & k_{N1}^{23} & \dots & k_{ND}^{23} \\ k_1^{31} & k_{11}^{32} & \dots & k_{1N}^{32} & k_{11}^{33} & \dots & k_{1D}^{33} \\ \vdots & \vdots & & \vdots & \vdots & & \vdots \\ k_D^{31} & k_{D1}^{32} & \dots & k_{DN}^{32} & k_{D1}^{33} & \dots & k_{DD}^{33} \end{bmatrix} \begin{Bmatrix} \{\Delta\} \\ \{\Delta^1\} \\ \vdots \\ \{\Delta^N\} \\ \{\bar{\Delta}^1\} \\ \vdots \\ \{\bar{\Delta}^D\} \end{Bmatrix} = \begin{Bmatrix} \{q\} \\ \{q^1\} \\ \vdots \\ \{q^N\} \\ \{\bar{q}^1\} \\ \vdots \\ \{\bar{q}^D\} \end{Bmatrix} \tag{18a}$$

where

$$\begin{aligned} \{\Delta\}^T &= \{u_1, v_1, w_1, \dots, u_m, v_m, w_m\} \\ \{\Delta^I\}^T &= \{u_1^I, v_1^I, \dots, u_m^I, v_m^I\} \\ \{\bar{\Delta}^I\}^T &= \{U_1^I, V_1^I, W_1^I, \dots, U_m^I, V_m^I, W_m^I\} \end{aligned} \tag{18b}$$

and the submatrices $[k^{11}]$, $[k_j^{12}]$, $[k_j^{21}]$, $[k_{jr}^{22}]$, $[k_{jr}^{23}]$, $[k_{rj}^{32}]$, $[k_{rs}^{33}]$ with $i, j = 1, \dots, N$ and $r, s = 1, \dots, D$ are given in Barbero (1989). The load vectors $\{q\}$, $\{q^1\} \dots \{q^N\}$, and $\{\bar{q}^1\}, \dots, \{\bar{q}^D\}$ are analogous to $\{\Delta\}$, $\{\Delta^1\}, \dots, \{\Delta^N\}$ and $\{\bar{\Delta}^1\}, \dots, \{\bar{\Delta}^D\}$, respectively [see eqn (18b)]. The nonlinear algebraic system is solved by the Newton–Raphson algorithm. The components of the Jacobian matrix are also given in Barbero (1989).

The nonlinear equations are linearized to formulate the eigenvalue problem associated with bifurcation (buckling) analysis:

$$([K_D]-\lambda[K_G])\cdot\Phi=0 \tag{19}$$

where $[K_D]$ is the linear part of the direct stiffness matrix and $[K_G]$ is the geometric stiffness matrix.

4. NUMERICAL RESULTS

Several examples are presented in order to validate the proposed formulation. Analytical solutions can be developed for simple cases and they are used for comparison with the more general approach presented here.

4.1. *Square thin film delamination*

A thin layer delaminated from an isotropic square plate (flexural rigidity, D) by a concentrated load P at its center is considered. The delamination is also assumed to be square with side $2a$. The base laminate is assumed to be rigid with respect to the thin delaminated layer. An analytical solution for the linear deflection and strain energy release rate can be derived assuming that the delaminated layer is clamped to the rigid base laminate. Due to the biaxial symmetry, a quadrant of the square delamination is analyzed using 2×2 and 5×5 meshes of nine-node elements. Either the clamped boundary condition is imposed on the boundary of the delamination or an additional band of elements with a closed delamination is placed around the delaminated area to simulate the nondelaminated region. Both models produce consistent results for transverse deflections and average strain energy release rates. A fine mesh is necessary to obtain a smooth distribution of the strain energy release rate G along the boundary of a square delamination. The linear solution for $P=10$ compares well with the analytical solution (see Fig. 1). The linear and nonlinear maximum delamination opening W and average strain energy release rate G_{av} as a function of the applied load P are shown in Fig. 2. It is evident that the membrane stresses caused

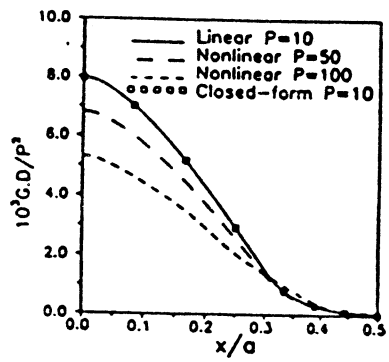

Fig. 1. Distribution of the strain energy release rate along the boundary of a square delamination due to concentrated load.

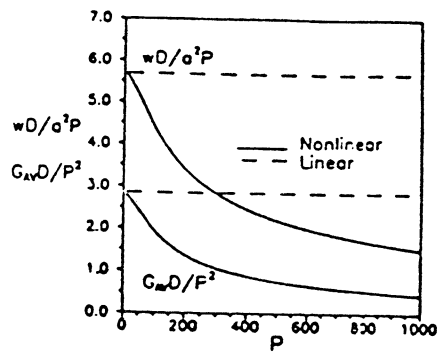

Fig. 2. Maximum delamination opening W and average strain energy release rate according to nonlinear analysis of a square delamination.

by the geometric nonlinearity reduce the magnitude of the average strain energy release rate considerably (Whitcomb and Shivakumar, 1987).

4.2. *Thin film cylindrical buckling*

In this example we consider an isotropic thin layer delaminated from a thick plate in its entire width. Due to symmetry, only one half of the length of the plate strip is modeled with the cylindrical bending assumptions and a nonuniform mesh of seven elements. The cylindrical bending assumption is satisfied by restraining all degrees of freedom in the y-direction. The base laminate is considered to be much more rigid than the thin delaminated layer so that it will not buckle or deflect during the postbuckling of the delaminated layer. First, an eigenvalue (buckling) analysis is performed to obtain the buckling load and corresponding mode shape. Then a nonlinear solution for the postbuckling configuration is sought. Excellent agreement is found in the jump discontinuity displacements U and W across the delamination. The values of delamination opening W and strain energy release rate G are shown in Figs 3 and 4 as a function of the applied load, where ε_{cr} is the critical strain at which buckling occurs for a delamination length of $2a$ (see Yin, 1988).

4.3. *Axisymmetric circular delamination*

Axisymmetric buckling of a circular, isotropic, thin-film delamination can be reduced to a one-dimensional boundary-value problem by means of the classical plate theory (CPT). One quadrant of a square plate of total width $2b$ with a circular delamination of radius a

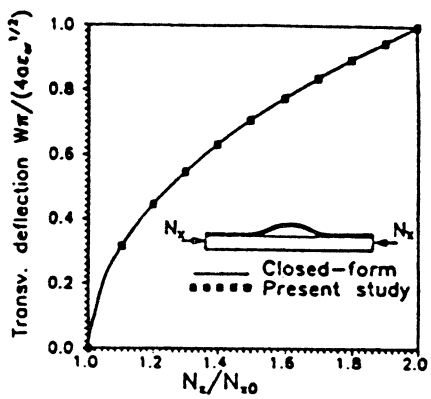

Fig. 3. Maximum delamination opening W for a thin film buckled delamination.

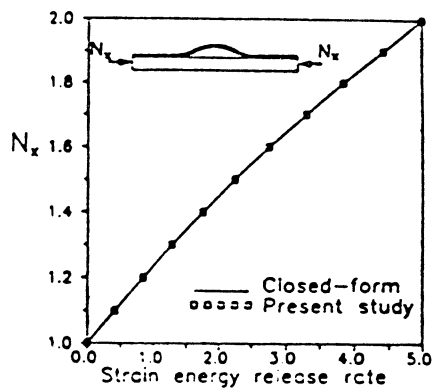

Fig. 4. Strain energy release rate for buckled thin film delamination.

is modeled. The layer-wise elements are capable of representing discontinuities of the displacements at the interface between layers. The symmetry boundary conditions used are:

$$u(0, y) = u^j(0, y) = U^j(0, y) = 0$$
$$v(x, 0) = v^j(x, 0) = V^j(x, 0) = 0$$

with $i = 1, \ldots, N$ and $j = 1, \ldots, D$; where N is the number of layers and D is the number of delaminations through the thickness; in this example, we have $D = 1$. The boundary of the delamination is specified by setting the jump discontinuity variables U^j, V^j and W^j to zero on the boundary of the delamination and wherever the plate is not delaminated. The boundary of the plate is subjected to the following boundary conditions, which produce a state of axisymmetric stress on the circular delamination:

$$u^j(b, y) = U^j(b, y) = 0; N_x(b, y) = -\hat{N}$$
$$v^j(x, b) = V^j(x, b) = 0; \; N_y(x, b) = -\hat{N}$$

where $\hat{N}$ is a uniformly distributed compressive force per unit length. The same material properties are used for the delaminated layer of thickness t and for the substrate of thickness $(h - t)$. To simulate the thin-film assumptions, a ratio $h/t = 100$ is used. First an eigenvalue analysis is performed to obtain the buckling load and corresponding mode shape. Then a Newton–Raphson solution for the post-buckling is sought. The Jacobian derivative method (see Barbero and Reddy, 1990) is used at equilibrium solution to compute the distribution of the strain energy release rate $G(s)$ along the boundary of the delamination. For this example, $G(s)$ is a constant. Its value, shown in Fig. 5 as a function of the applied load, is in excellent agreement with the approximate analytical solution (see Yin, 1985).

4.4. *Circular delamination under unidirectional load*

In this example we analyze a circular delamination, centrally located in a square plate of total width $2c$ and subjected to a uniformly distributed in-plane load N_x. The example is considered because results of a three-dimensional analysis are available (Whitcomb, 1988) in the literature. Compared to the last example, this problem does not admit an axisymmetric solution. Therefore, the distribution $G(s)$ varies along the boundary of the delamination. A quasi-isotropic laminate $[\pm 45/0/90]$ of total thickness $h = 4$ mm and a circular delamination of diameter $2a$ located at $z = 0.4$ mm is considered. The material properties used are those of AS4/PEEK: $E_1 = 134$ GPa, $E_2 = 10.2$ GPa, $G_{12} = 5.52$ GPa, $G_{23} = 3.43$ GPa, $\nu_{12} = 0.3$. As is well known, the quasi-isotropic laminate exhibits equivalent isotropic

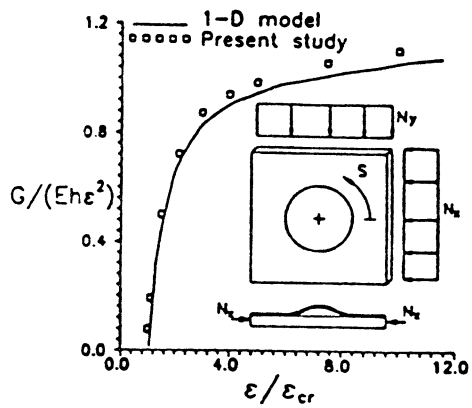

Fig. 5. Strain energy release rate for a buckled thin film, axisymmetric delamination as a function of the in-plane load.

behavior when loaded in its plane. The bending behavior, however, depends on the orientation. To avoid complications in the interpretation of the results introduced by the non-isotropic bending behavior, an equivalent isotropic material is used by Whitcomb (1988), where the equivalent stiffness components of the 3-D elasticity are found from the relation:

$$\bar{C}_{ij} = \frac{1}{8}\sum_{k=1}^{N} (C_{ij})^k.$$

Due to the transverse incompressibility used in this work, it is more convenient and customary to work with the reduced stiffness. Equivalent material properties can be found directly from the A-matrix of the quasi-isotropic laminate as follows. First, compute the equivalent reduced stiffness coefficients

$$Q_{ij} = A_{ij}/h,$$

where h is the total thickness of the plate and A_{ij} are the extensional stiffnesses. Next, the equivalent material properties can be found as:

$$E_{11} = Q_{11} - Q_{22}$$

$$E_{22} = Q_{22}\left(1 - \frac{Q_{22}}{Q_{11}}\right)$$

$$G_{12} = Q_{33}$$

$$G_{23} = Q_{55}$$

$$\nu_{12} = \frac{Q_{11}E_{11} - E_{11}^2}{Q_{11}E_{22}}.$$

An eigenvalue analysis reveals that the delaminated portion of the plate buckles at $N_x = 286{,}816$ N m^{-1} for $a = 15$ mm and at $N_x = 73{,}666$ N m^{-1} for $a = 30$ mm. The maximum transverse opening of the delamination as a function of the applied in-plane strain ε_x is shown in Fig. 6. The differences observed with the results of Whitcomb (1988) are due to the fact that in the latter an artificially zero transverse deflection is imposed on the base laminate to reduce the computational cost of the three-dimensional finite element solution. The differences are more important for $a = 30$ mm, as indicated by the dashed line in Fig. 6, which represents the transverse deflection w of the midplane of the plate. The square symbols denote the total opening (or gap) of the delamination, while the solid line represents the opening reported by Whitcomb (1988) with $w = 0$. The differences in the

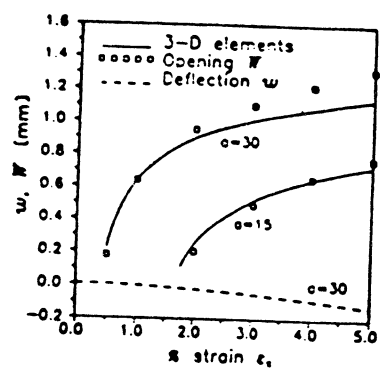

Fig. 6. Maximum transverse opening W of a circular delamination of diameter $2a$ in a square plate subjected to in-plane load N_x as a function of the in-plane uniform strain.

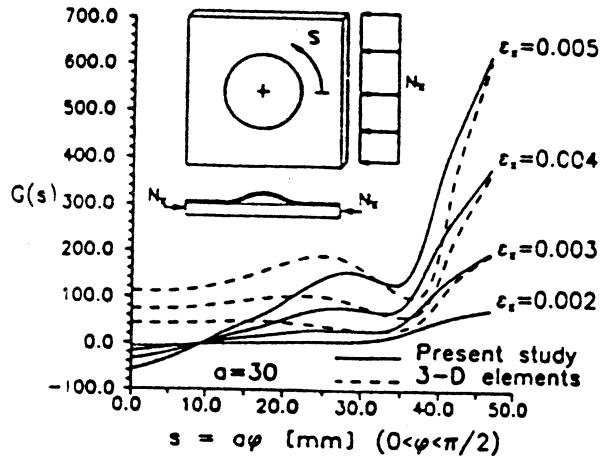

Fig. 7. Distribution of the strain energy release rate along the boundary of a circular delamination for various values of the applied in-plane axial strain.

total opening W and transverse deflection w have an influence on the distribution of the strain energy release rate, as can be seen in Fig. 7. Both solutions (i.e., solutions of 3-D elements and the present 2-D elements) coincide for the small delamination of radius $a = 15$ mm, as shown in Fig. 8. For the larger radius $a = 30$ mm, the assumption $w = 0$ is no longer valid, and differences can be observed in Fig. 8, although the maximum values of G coincide and the shapes of the distributions of G are quite similar. Mesh refinement, with at least two elements close to the delamination boundary, must be used to account for the sudden changes in deflections and slope in a narrow region close to the delamination boundary, similar to the phenomena described by Bodner (1954). Distributions of the strain energy release rates $G(s)$ along the boundary of the delamination are shown in Figs 7 and 8 for the different delamination radii, $a = 15$ mm and $a = 30$ mm, respectively. The value $s = 0$ corresponds to $(x = a, y = 0)$ and $s = a\pi/2$ to $(x = 0, y = a)$. Negative values of $G(s)$ indicate that energy should be provided to advance the delamination in that direction. Negative values are obtained as a result of delaminated surfaces that come in contact, thus eliminating the contribution of mode I of fracture but not of modes II and III. The present analysis does not include contact constraints and therefore layers may overlap. As noted by Whitcomb (1988), the strain energy release rate $G(s)$ in the region without overlap is not significantly affected by imposing contact constraints on the small overlap area.

4.5. *Unidirectional delaminated graphite–epoxy plate*

A circular delamination of radius $a = 5$ in. in a square plate of side $2c = 12$ in., made of unidirectional graphite–epoxy, is considered next. The thickness of the plate is $h = 0.5$

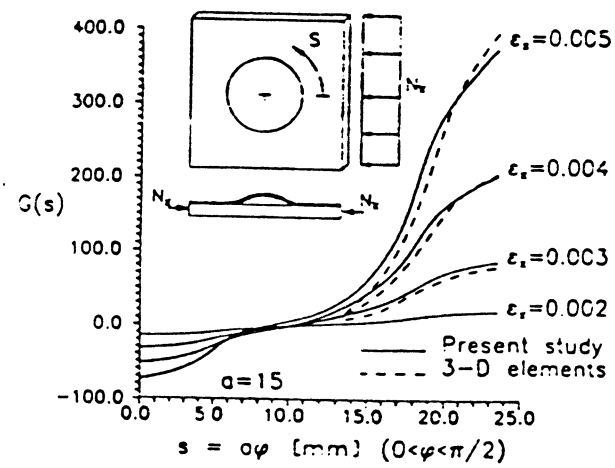

Fig. 8. Distribution of strain energy release rate along the boundary of a circular delamination for various values of in-plane axial strain.

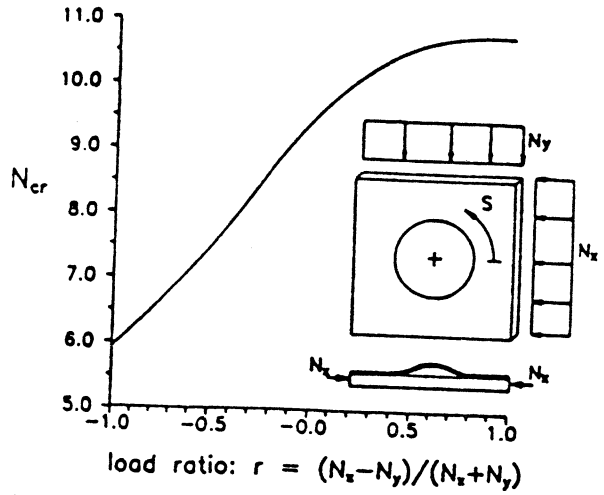

Fig. 9. Buckling load versus the ratio of in-plane loads N_x and N_y for a circular delamination.

in., and the delamination is located at a distance $t = 0.005$ in. from the surface. An eigenvalue analysis is used to obtain the magnitude of the in-plane load under which the thin delaminated layer buckles. Due to the orthotropic nature of the material used in this example, it is interesting to study the effect of different combinations of loads N_x and N_y. Let us denote the load ratio as

$$r = \frac{N_x - N_y}{N_x + N_y}.$$

The magnitude of the buckling load as a function of the load ratio r, with $-1 < r < 1$, is shown in Fig. 9. The distribution of the strain energy release rate $G(s)$ along the boundary $s = a\phi$, $0 < \phi < \pi/2$ is plotted in Figs 10–12 for the load ratios of $r = -1$, 0, and 1, and for several values of the applied in-plane load, in multiples λ of the buckling load N_{cr}. For $r = 1$ (i.e., $N_x = N$ and $N_y = 0$) it is clear that (see Fig. 10) the delamination is likely to propagate in a the direction approximately perpendicular to the load direction. Introduction of load in the direction perpendicular to fibers causes the maximum value of G to align closer to the x-axis. Note that both the magnitude and the shape of the distribution of $G(s)$ change as the load ratio changes (see Fig. 13). The plots suggest that the propagation or arrest of delaminations is greatly influenced by the anisotropy of the material and the dominant load.

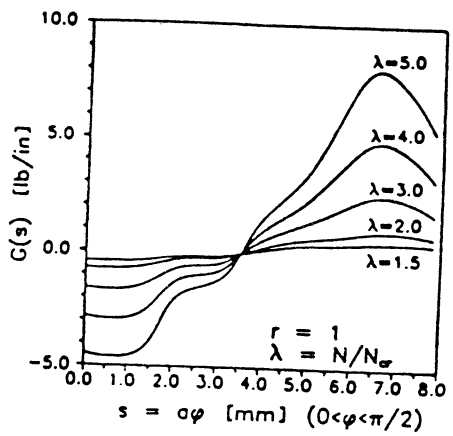

Fig. 10. Distribution of the strain energy release rate along the boundary of a circular delamination for various values of applied load N.

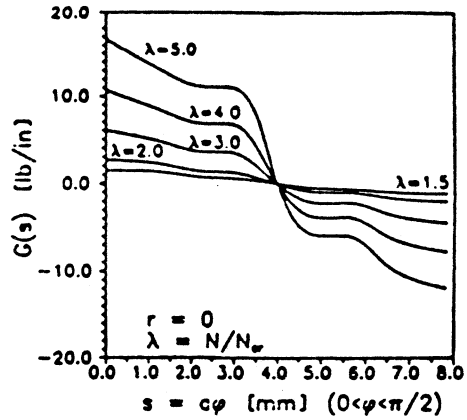

Fig. 11. Distribution of the strain energy release rate along the boundary of a circular delamination for the ratio $r = 0$.

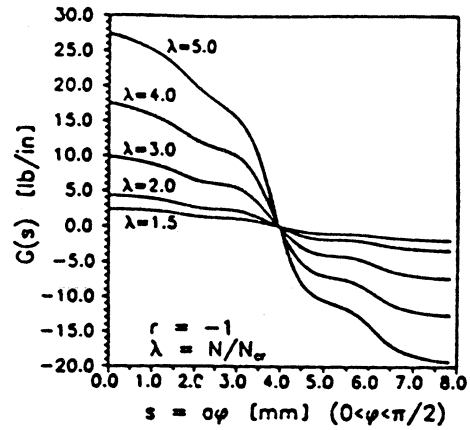

Fig. 12. Distribution of the strain energy release rate along the boundary of a circular delamination for the ratio $r = -1$.

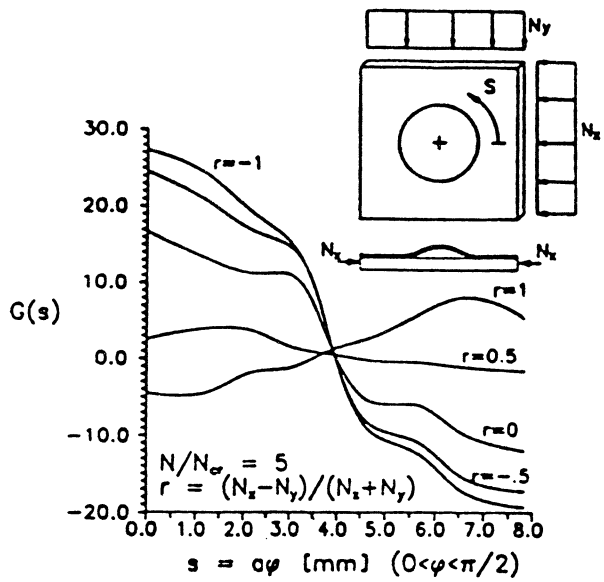

Fig. 13. Distribution of the strain energy release rate along the boundary of a circular delamination of radius $a = 5$ in. for various values of the load ratio, r.

5. SUMMARY AND CONCLUSIONS

A layer-wise theory and associated finite-element model for the study of delaminations in laminated composite plates is developed. The same displacement distribution in the individual layers is capable of representing displacement discontinuity conditions at interfaces between layers. The finite element model predicts accurate distributions of strain energy release rates along the boundary of delaminations of arbitrary shape. The model can be used to study multiple delaminations through the thickness of the plate.

The layer-wise laminate plate theory provides an adequate framework for the analysis of laminated composite plates. Particularly, the layer-wise linear approximation of the displacements through the thickness and the use of Heaviside step functions to model delaminations prove to be an effective approach for an accurate analysis of local effects in laminated composite plates. It must be noted, however, that the computational cost of the proposed analysis makes it unattractive for prediction of global behavior when compared with conventional theories. For the prediction of local effects (i.e., delaminations, interlaminar stresses, etc.), the theory and formulation presented in this study shows its potential as an alternative to three-dimensional analysis. The model can also be used in a global–local analysis scheme wherein the local regions are modeled using the layer-wise theory and global regions are modeled using less refined theories, say the first-order laminate theory. Transition elements must be developed to join regions modeled by the layer-wise theory to regions modeled by less expensive theories in global–local analysis procedures.

It is expected that accurate stress distributions obtained with this type of analysis, along with meaningful failure theories, will enable realistic prediction of failure initiation and propagation in composite laminates. Also, the layer-wise plate theory can be used as a post-processor to enrich the stress prediction of the first-order shear deformation theory.

Acknowledgements—The support of this work by NASA Langley Research Center and the U.S. Army through Grant NAG-1-1030 and by NSF International Programs (U.S.–India Cooperative Science Program) through Grant INT-8908307 is gratefully acknowledged.

REFERENCES

Ashizawa, M. (1981). Fast interlaminar fracture of a compressively loaded composite containing a defect. *Fifth DOD–NASA Conf. on Fibrous Composites in Structural Design*, New Orleans, LA.

Barbero, E. J. (1989). On a generalized laminate theory with application to bending, vibration, and delamination buckling in composite laminates. Ph.D. Dissertation, Virginia Polytechnic Institute and State University, Blacksburg, VA.

Barbero, E. J. and Reddy, J. N. (1990). The Jacobian derivative method for three-dimensional fracture mechanics. *Commun. Appl. Numer. Meth.* 6(7), 507–518.

Barbero, E. J., Reddy, J. N. and Teply, J. L. (1990a). A general two-dimensional theory of laminated cylindrical shells. *AIAA J.* 28(3), 544–552.

Barbero, E. J., Reddy, J. N. and Teply, J. L. (1990b). An accurate determination of stresses in thick laminates using a generalized plate theory. *Int. J. Numer. Meth. Engng* 29, 1–14.

Bodner, S. R. (1954). The post-buckling behavior of a clamped circular plate. *Q. Appl. Math.* 12, 397–401.

Bottega, W. J. and Maewal, A. (1983). Delamination buckling and growth in laminates. *J. Appl. Mech.* 50, 184–189.

Chai, H. (1982). The growth of impact damage in compressively loaded laminates. Thesis, California Institute of Technology.

Chai, H. and Babcock, C. D. (1985). Two-dimensional modelling of compressive failure in delaminated laminates. *J. Compos. Mater.* 19, 67–98.

Chai, H., Babcock, C. D. and Knauss, W. G. (1981). One dimensional modelling of failure in laminated plates by delamination buckling. *Int. J. Solids Structures* 17, 1069–1083.

Durocher, L. L. and Solecki, R. (1975). Steady-state vibrations and bending of transversely isotropic three-layer plates. *Developments in Mechanics, Proc. 14th Midwestern Mech. Conf.*, Vol. 8, pp. 103–124.

Fei, Z. and Yin, W.-L. (1985). Axisymmetric buckling and growth of a circular delamination in a compressed laminate. *Int. J. Solids Structures* 21, 503–514.

Inoue, I. and Kobatake, Y. (1959). Mechanics of adhesive joints, part IV: Peeling test. *Appl. Scient. Res.* 8A, 321.

Kachanov, L. M. (1976). Separation failure of composite materials. *Polymer Mech.* 12, 812–815.

Mau, S. T. (1973). A refined laminated plate theory. *J. Appl. Mech.* 40, 606–607.

Murakami, H. (1986). Laminated composite plate theory with improved in-plane responses. *J. Appl. Mech.* 53, 661–666.

Obreimoff, J. W. (1980). The splitting strength of Mica. *Proc. R. Soc.* A127, 290.

Reddy, J. N. (1984). *Energy and Variational Methods in Applied Mechanics*. John Wiley, New York.

Reddy, J. N. (1987). A generalization of two-dimensional theories of laminated plates. *Commun. Appl. Numer. Meth.* **3**, 113–180.
Reddy, J. N. (1988). Mechanics of composite structures. In *Finite Element Analysis for Engineering Design* (Edited by J. N. Reddy, C. S. Krishna Moorthy and K. N. Seetharamu), Chap. 14, pp. 338–359. Springer, Berlin.
Reddy, J. N. (1989). On refined computational models of composite laminates. *Int. J. Numer. Meth. Engng* **27**, 361–382.
Reddy, J. N. (1990). A review of refined theories of laminated composite plates. *Shock Vibr. Digest* **22**(7), 3–17.
Reddy, J. N., Barbero, E. J. and Teply, J. L. (1989). A plate bending element based on a generalized laminate plate theory. *Int. J. Numer. Meth. Engng* **28**, 2275–2292.
Sallam, S. and Simitses, G. J. (1985). Delamination buckling and growth of flat, cross-ply laminates. *Comput. Struct.* **4**, 361–381.
Seide, P. (1980). An improved approximate theory for the bending of laminated plates. *Mech. Today* **5**, 451–466.
Shivakumar, K. N. and Whitcomb, J. D. (1985). Buckling of a sublaminate in a quasi-isotropic composite laminate. *J. Compos. Mater.* **19**, 2–18.
Simitses, G. J., Sallam, S. and Yin, W. L. (1985). Effect of delamination of axially loaded homogeneous laminated plates. *AIAA J.* **23**, 1437–1440.
Srinivas, S. (1973). Refined analysis of composite laminates. *J. Sound Vibr.* **30**, 495–507.
Sun, C. T. and Whitney, J. M. (1972). On theories for the dynamic response of laminated plates. AIAA Paper No. 72-398.
Toledano, A. and Murakami, H. (1987). A composite plate theory for arbitrary laminate configurations. *J. Appl. Mech.* **54**, 181–189.
Webster, J. D. (1981). Flaw critically of circular disbond defects in compressive laminates. CCMS Report 81-03.
Whitcomb, J. D. (1981). Finite element analysis of instability related delamination growth. *J. Compos. Mater.* **15**, 113–180.
Whitcomb, J. D. (1988). Instability-related delamination growth of embedded and edge delaminations. NASA TM 100655.
Whitcomb, J. D. and Shivakumar, K. N. (1987). Strain-energy release-rate analysis of a laminate with a post-buckled delamination. NASA TM 89091.
Wilt, T. E., Murthy, P. L. N. and Chamis, C. C. (1988). Fracture toughness computational simulation of general delaminations in fiber composites. AIAA Paper 88-2261, pp. 391–401.
Yin, W.-L. (1985). Axisymmetric buckling and growth of a circular delamination in a compressed laminate. *Int. J. Solids Structures* **21**, 503–514.
Yin, W.-L. (1988). The effects of laminated structure on delamination buckling and growth, *J. Compos. Mater.* **22**, 502–517.
Yu, Y. Y. (1959). A new theory of elastic sandwich plates—one dimensional case. *J. Appl. Mech.* **26**, 415–421.